The cooling rate of the heated vapor compression cycle in case of using refrigerants R134a, R22, and R600a

MOHAMED SALAMA ABD-ELHADY[a*]
EMMANOUEIL BISHARA MELAD[b]
MOHAMED ABD-ELHALIM[c]
SEIF ALNASR AHMED[a]

Mechanical Engineering Department, Faculty of Engineering, Beni-Suef University, Sharq El-Nile, New Beni-Suef, 62521 Beni-Suef, Egypt

Faculty of Technology and Education, Beni-Suef University, Sharq El-Nile, New Beni-Suef, 62521 Beni-Suef, Egypt

Faculty of Technology and Education, Suez University, 43527 Suez, Egypt

Abstract The most power consuming part in the vapor compression cycle (VCC) is the gas compressor. Heating the refrigerant under constant volume after the compressor increases the condenser pressure, which con-sequently increases the cooling rate of the VCC. This study examined the influence of heating different refrigerants, *i.e.* R143a, R22, and R600a on the cooling rate of the VCC. Four experiments have been performed: the first experiment is a normal VCC, *i.e.* without heating, while in the second, third, and fourth experiments were carried out to raise the temperature of the refrigerant to 50˚C, 100˚C, and 150˚C. It has been found that heating raises the refrigerant pressure in VCC and thereby improves the refriger-ant's mass flow rate resulting in an improvement in the cooling power for the same compressor power. Heating the refrigerant after the mechanical compressor increases the temperature of the condenser as well as the tem-perature of the evaporator when using refrigerant R134a, which prevents the refrigeration cycle to be used in freezing applications, however using re-frigerant R22 or refrigerant R600a promotes the heated VCC to be used in

freezing applications. Refrigerant R600a has the lowest operating pressure compared to R134a and R22, which promotes R600a to be used rather than R134a and R22 from a leakage point of view.

Keywords: Compression cycle; Power saving; Refrigerant; Refrigerating cycle; Cooling rate

Nomenclature

c	–	specific heat of water, kJ/kg°C
COP	–	coefficient of performance
h_1	–	enthalpy of the refrigerant at the beginning of the compression process
h_2	–	enthalpy of the refrigerant at the end of the compression process
h_3	–	enthalpy of the refrigerant at the inlet to the expansion valve
h_4	–	enthalpy of the refrigerant at the exit of the expansion valve
m_{water}	–	mass of water, kg
$\dot{m}_{ref}$	–	mass flow rate of the refrigerant, kg/s
$\dot{Q}_L$	–	cooling rate, kW
$\dot{Q}_{comp}$	–	heating power during the compression process, kW
Q_{water}	–	heat transfer rate of the water, kW
P	–	pressure, hPa
T	–	temperature, °C
T_s	–	temperature of the refrigerant in the storage tank, °C –
t_c		cooling time, s
$\dot{W}$	–	work, kJ
$\dot{W}_{comp}$	–	mechanical compression, kW
Δh_{comp}	–	enthalpy change during the entire compression process, = $h_2 - h_1$, kJ/kg
Δh_{evap}	–	enthalpy change across the evaporator, = $h_1 - h_4$, kJ/kg
$\Delta\dot{m}_{ref}$	–	percentage increase in the mass flow rate
$\Delta\dot{Q}_L$	–	percentage increase in the cooling rate
ΔT	–	temperature difference, °C

Subscripts

1	–	state of the refrigerant at the exit of the evaporator
2	–	state of the refrigerant at the exit of the compression process
3	–	state of the refrigerant at the inlet to the expansion valve
4	–	state of the refrigerant at the exit of the expansion valve
L	–	low
comp	–	compression
evap	–	evaporator
ref	–	refrigerant

Abbreviations

Al_2O_3	–	aluminum oxide
VCC	–	vapor compression cycle

1 Introduction

Refrigeration and air conditioning consume large amounts of electrical energy, which the compressor mainly consumed to run the refrigeration cycle. The International Institutes of Refrigeration submitted a field study stat-ing that the total number of air conditioning systems and heat pumps for refrigeration equipment is around 5 billion are operated worldwide, which consumes about 20% of all electricity used in the whole world [1,2]. Therefore, continuous efforts are exerted to increase the performance efficiency of these systems [3–5], because even relatively small improvements in their performance can have a major impact on energy consumption [6–8]. This affects the cost associated with the performance and maintenance of these units and the improvement of their performance.

The most common refrigeration cycle is the vapor compression cycle (VCC) which includes four main components, i.e. compressor, condenser, expansion valve, and evaporator. The refrigerant is compressed in the compressor to a higher temperature and pressure, and then it releases its heat energy into the surrounding environment through the condenser. The condensed refrigerant is then expanded in an expansion valve to lower the temperature and pressure of the refrigerant. The refrigerant then enters the evaporator to absorb heat from the refrigerated space. Then the re-frigerant returns to the compressor and the cycle continues. Therefore, the performance of the cooling systems can be explained by the coefficient of performance, which is the ratio between the rate of cooling, $\dot{Q}_L$, and the compressor power, $\dot{W}_{comp}$,

$$\mathrm{COP} = \frac{\dot{Q}_L}{\dot{W}_{comp}} . \tag{1}$$

Many researchers have made improvements to minimize power consump-tion, $\dot{W}_{comp}$, and to increase the refrigeration effect, $\dot{Q}_L$, in the vapor com-pression refrigeration system. Yin *et al.* [9] presents a cascade control strat-egy for the VCC systems to improve the energy consumption and fulfill the cooling requirements of indoor occupants simultaneously. It has been found that the proposed cascade control strategy can improve energy efficiency by up to 5.8%. The influence of aluminum oxide (Al_2O_3) nanoparticles on thermophysical characteristics has been studied by Alawi *et al.* [10] where 1 to 4% by volume of Al_2O_3 nanoparticles were present in the refriger-ant R141b at a temperature from 10 to 35°C. It is found that the im-provement in the density, dynamic viscosity and the thermal conductivity

of the Al_2O_3/R-141b nano-refrigerant are approximately 11.54%, 12.63%, and 28.88%, respectively, combined with the basic refrigerant (R141b) for a similar volume fraction and temperature of 4% vol. and 35°C. Ahmed *et al.* [11] investigated experimentally the performance of a chilled water air conditioner with and without alumina nanofluids. Al_2O_3 nanoparticles were added with water to the cooling tank using various concentrations i.e. 0.1, 0.2, 0.3, and 1% by weight. Alumina nanofluids were continuously supplied to the cooling coil. It has been found that less time is reached to obtain the desired child fluid temperature for all the different concen-trations of nanofluids (Al_2O_3-water) compared to pure water. The results also showed a decrease in energy consumption and an increase in cooling capacity, which in turn increases the efficiency by around 5% and by 17% for a concentration of aluminum oxide nanoparticles of 0.1% and 1% by weight, respectively.

Many researches have tried to improve the performance of the vapor compression cycle [12, 13]. Patel *et al.* [14] discussed ways to improve the performance of the VCC through beneficial refrigerant overheating before entering the compressor. The working conditions were the pressure in the condenser and the evaporator of 720 kPa and 220 kPa, respectively. The R12 is used as a refrigerant and an overheating of 10°C is applied. The analysis showed how it is possible to increase the performance of vapor compression systems due to the beneficial overheating that occurs in the evaporator to create an additional cooling effect. Overheating of the re-frigerant also guarantees safe operation of the compressor. Cui *et al.* [15] proposed a modification of the VCC by adding a separator at the con-denser outlet to minimize the supply of steam to the evaporator at a low temperature. The cycle model has been developed and confirmed by ex-perimental data with an accuracy of 10%. Theoretical studies of the new cycle decided that the efficiency and the volumetric cooling capacity are respectively improved by 7.7% and 5.5% compared to a conventional con-denser under nominal conditions. Qureshi and Bhatt studied the COP of the vapor compression cycle using refrigerants R134a and R600a [16]. The results showed that the COP of the vapor compression cycle using R600a is more than that of the vapor compression cycle using R134a in optimum conditions. Also, the amount of charge requirement for R600a was lower than for R134a which not only offered economic benefits but also significantly reduced the probability of hydrocarbon refrigerant ig-nition. The new configuration of the vapor compression-absorption inte-grated refrigeration system (VCAIRS) was analyzed by Jain *et al.* [17].

The proposed configuration operates at a generator temperature below 60°C. Thus, the use of low quality residual heat for its operation is authorized. The performance of vapor compression-absorption integrated refrigeration system is also compared to the equivalent vapor compression refrigeration system (VCRS) for the same cooling capacity of 100 kW. In addition, the preliminary energy analysis shows that 35.2% of the total vapor compression-absorption integrated refrigeration system irreversibility index can be avoided by improving the performance of the system components. Bellos *et al.* [18] proposed a new solar-assisted mechanical compression refrigeration system. Evacuated tube collectors are used to partially compress the thermal refrigerant after a mechanical compressor us-ing R404a. This system is analyzed using an Engineering Equation Solver (EES) software under stationary conditions [19]. This is established that the optimal pressure values after the mechanical compressor are 75% of the maximum, and in this case, energy savings can be achieved from 15% to 25%. However, Bellos *et al.* [20] proposed a new modification to the mechanical compression developed using solar panels [21–24], with the aim of increasing the effectiveness of the VCC. The suggested compression process takes place in two stages, the first stage of compression is carried out with a compressor, and then the gas is cooled by an intercooler, then the second compression step produced by electric heating at constant vol-ume. It is established that CO_2 and R32 are the most promising refrig-erants in the proposed cycle with a COP of 1.492 and the exergy effi-ciency 41.01%.

Compressor suction pressure is higher with an ejector than it would be in a standard cycle using the expansion valve, which reduces working compression and increases the system efficiency [25–31]. Sanaya *et al.* [32] tried to increase the efficiency of a simple refrigeration cycle with steam-steam ejector. The ejector evaporator refrigeration cycle is combined with the ejector evaporator simple refrigeration cycle. Three different refrigerants for the vapor ejection cycle and four different refrigerants for the liquid-vapor ejection cycle, two refrigerants are also selected for the combined cycle of vapor and liquid ejectors at the optimum point. An analysis of the proposed new cycle shows 18% higher efficiency, a 25% higher exergy efficiency, a 31% lower energy consumption, and an 8% lower annual cost for the specific cooling capacity.

From this review of literature, it can be concluded that there are many methods that are used to minimize compression work and increase the efficiency of the VCC. The aim of this study is to increase the VCC cooling rate

for the same compressor work applied, and this is done by heating the refrigerant that leaves the compressor under constant volume. The proposed cycle is similar to the VCC except that the compression processes is carried out in two stages, the first stage is carried out through a gas compressor, and in the second stage heating the refrigerant at a constant volume. The newly developed cycle will be called the heated vapor compression cycle (HVCC). The heating process can be carried out using electric heaters or using solar collectors. An experimental configuration has been developed to study the effect of heating the refrigerant in a VCC. Four experiments are carried out; the first experiment is a normal VCC, *i.e.* without heat-ing, while in the second, third, and fourth experiments, the refrigerant was heated to 50°C, 100°C, and 150°C, respectively. The refrigeration cycle is examined under three different refrigerants R134a, R22, and R600a. De-spite the fact that R22 has been banned, it has been examined in the experiments for the sake of comparison and assurance of the influence of heating the refrigerant on the cooling rate. The experimental configuration used in this study and the experimental procedure are explained in the next section, followed by experimental results and discussion, and subsequently conclusions.

2 Experimental setup

The designed refrigeration vapor compression system consists of five components that is compressor, storage tank, condenser, capillary tube, and an evaporator, which are connected in series as shown in Fig. 1. The compressor takes the refrigerant from the evaporator to compresses it and then to the storage tank. An electric heater is used to heat the refrigerant in the storage tank. The refrigerant pressure increases due to heating at a constant volume by the electric heater. The electric heater is used to simulate a parabolic solar collector heat-pipe due to its stable operation [33–37], which can be used to conduct experiments independent of the intensity of the sun. The temperature of the refrigerant inside the storage tank is controlled by a thermostat, such that when the temperature of the refrig-erant reaches a predefined set temperature the thermostat shuts down the heater. A pressure relief valve is connected at the exit of the storage tank as a safety valve, such that it opens when the pressure inside the storage tank reaches 600 kPa, however, due to the fact that the storage tank is in a closed cycle, so, heating inside the storage tank can increase the pressure

to become higher than 600 kPa even if the valve is completely opened. The pressure of the refrigerant after the mechanical compressor in case of no heating is higher than 600 kPa, which causes the relief valve to be always opened during all of the performed experiments, *i.e.* with or without heat-ing. Then the refrigerant enters the condenser in which it is cooled and transformed into a saturated liquid. The refrigerant pressure decreases due to the capillary tube and then enters the evaporator.

The compressor has a power of 186.4 W. The storage tank has a diameter of 0.18 m and a height 0.19 m, in which the refrigerant is heated by an electric heater of 300 W. The pressure relief valve can be adjusted to open at a certain pressure, allowing the refrigerant to flow to the condenser. A cross flow heat exchanger is used for the condenser with an external fan to increase the cooling rate of the refrigerant. The capillary tube diameter and its length are chosen according to the compressor, such that the diameter is 1.09 mm and the length is 3 m [38]. Pressure gauges are installed after the condenser and the evaporator, which are of the Bourdon type. A spiral evaporator is used, which has a diameter of 0.12 m and a total length of 5 m. The diameter of the tubes of the coil is 7 mm, and it is immersed in an insulated water tank. The walls of the tank are a sandwich panels

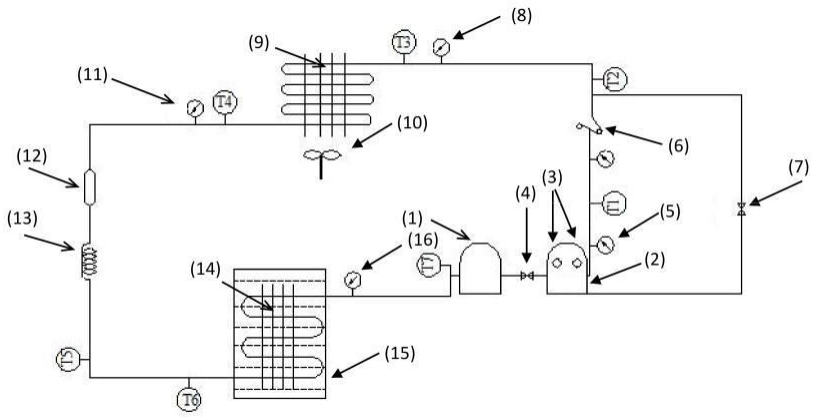

1 – Compressor
2 – Storage Tank
3 – Electrical Heaters
4 – Valve
5 – Pressure gauge
6 – Pressure relief valve
7 – Valve
8 – Pressure gauge
9 – Condenser
10 – Fan
11 – Pressure gauge
12 – Filter
13 – Capillary tube
14 – Evaporator
15 – Cold water tank
16 – Pressure gauge
17 – T1–T7 Thermocouples

Figure 1: Schematic diagram of the experimental setup.

filled with polystyrene foam. The water tank contains 6 kg of water, which is cooled to 9°C. The temperature inside the water tank is controlled by a thermostat, such that when the water temperature reaches 9°C, it stops the compressor and the cycle.

Water in the water tank is cooled by natural convection, and its temper-ature is measured by a type K thermocouple that is connected to a data acquisition card to store and retrieve data for later analysis. The refrig-erant temperature is measured at the following positions; (a) before and after the condenser, (b) before and after the evaporator, (c) after the re-frigerant storage tank and (d) inside the water tank, as shown in Fig. 1. All temperatures are measured with type K thermocouples. [39] which have an accuracy of ±1°C and are all connected to a PicoLog 1216 data acquisition card [40], for real-time measurement.

3 Experimental procedure

Four separate experiments were carried out for the tested refrigerants, which are R134a, R22, and R600a. The refrigerant in the first experiment is compressed using a gas compressor, and in the other three experiments, the refrigerant is compressed in two steps, first with a gas compressor then by heating the refrigerant under constant volume in the storage tank up to 50°C, 100°C, and 150°C, respectively. The water temperature is controlled by a thermostat, such that the refrigeration cycle continues until the tem-perature in the water tank drops to 9°C, then the cycle stops. The time of cooling the water to a predetermined temperature of 9°C is measured by the data acquisition systems.

4 Results and discussions

The aim of this research is to study the effect of heating the refrigerant after a compression process on the cooling rate of the vapor compression cycle as a function of the refrigerant type. Different refrigerant types are examined, *i.e.* R134a, R22, and R600a. Each refrigerant is heated to 50°C, 100°C, and 150°C. It has been concluded by Abd-Elhady *et al.* [41] that heating the refrigerant after the compressor under constant volume increases the pres-sure as well as the mass flow rate. The effect of heating the refrigerant after the compressor on the condenser pressure is shown in Table 1, while on the evaporator pressure is shown in Table 2, for the three types of refrigerants

Table 1: Effects of the heating process on the condenser pressure and temperature at outlet of the condenser for the examined three refrigerant types.

Experiment	R134a			R22			R600a		
	Press. (kPa)	Enthalpy, h_2 (kJ/kg)	Temp. (°C)	Press. (kPa)	Enthalpy, h_2 (kJ/kg)	Temp. (°C)	Press. (kPa)	Enthalpy, h_2 (kJ/kg)	Temp. (°C)
No heating	1039	322.1	23	1160	370.7	20	640	822.6	25
Heating, T_S = 50°C	1880	313.1	30	1440	362.9	25	880	812.7	29
Heating, T_S = 100°C	2010	315.2	35	1680	366.1	27	1040	795.4	32
Heating, T_S = 150°C	2100	315.8	38	1720	361.2	30	1060	797.1	34

Table 2: Effects of the heating process on the evaporator pressure and temperature at inlet of the evaporator for the three refrigerant types examined.

Experiment	R134a				R22				R600a			
	Press. (kPa)	*Temp., T_4 (°C)	**Enthalpy, $h_3 = h_4$ (kJ/kg)	Enthalpy, h_1 (kJ/kg)	Press. (kPa)	Temp., T_4 (°C)	Enthalpy, $h_3 = h_4$ (kJ/kg)	Enthalpy, h_1 (kJ/kg)	Press. (kPa)	Temp., T_4 (°C)	Enthalpy, $h_3 = h_4$ (kJ/kg)	Enthalpy, h_1 (kJ/kg)
No heating	130	–18.0	80.8	261.3	93	–28	68.9	265.1	66	–16	388.8	701.5
Heating, T_S = 50°C	270	–1.0	91.4	258.7	141	–23	82.7	265.7	107	–12	399.4	701.4
Heating, T_S = 100°C	289	0.0	98.0	260.0	150	–16	77.9	266.2	150	–9	407.2	700.8
Heating, T_S = 150°C	310	2.4	101.1	260.8	180	–14	81.7	267.0	162	–8	404.8	701.9

*The subscripts 4 and 1 stand for nodes 4 and 1 in the refrigeration cycle, which are at the inlet and outlet of the evaporator, respectively.

**The subscript 3 stands for node 3 in the refrigeration cycle, which is at the exit of the condenser.

that have been tested. The pressure values are the absolute pressure. The pressure-enthalpy ($P-h$) diagram of the refrigeration cycle in case of no heating and heating up to 50°C are shown in Fig. 2. The refrigeration cycle 1−2−3−4 is in case of no heating, while the cycle 1^0–2^0–3^0–4^0 is in case of heating the refrigerant up to 50°C. The other cycles, *i.e.* heating up to 100°C and 150°C, are not presented for the sake of simplicity and to avoid complexity in the figure. States (1) and (2) are the states of the refrigerant at the inlet and outlet of the compression process, respectively, while states (3) and (4) are the states of the refrigerant at the inlet and outlet of the expansion valve. State (2) is the final state at the end of the compression process, *i.e.* before the condenser. It can be inferred from Tables 1 and 2, and from Fig. 2 that the pressure of the condenser and the evaporator increases as the heating temperature increases, where the pressure of the condenser and the evaporator in case of using R600a are the lowest value in all refrigerants, but the pressure of the condenser and the evaporator in case of using R134a are the highest value in all refrigerants. The inlet temperature of the evaporator in case of using R22 is the lowest value in all refrigerants; however, the inlet temperature of the evaporator in case of using R134a is the highest value in all refrigerants. The condenser pressure in the case of R134a has reached 2100 kPa in case of heating the refrigerant up to 150°C, however, it has reached 1060 kPa in case of R600a, which is

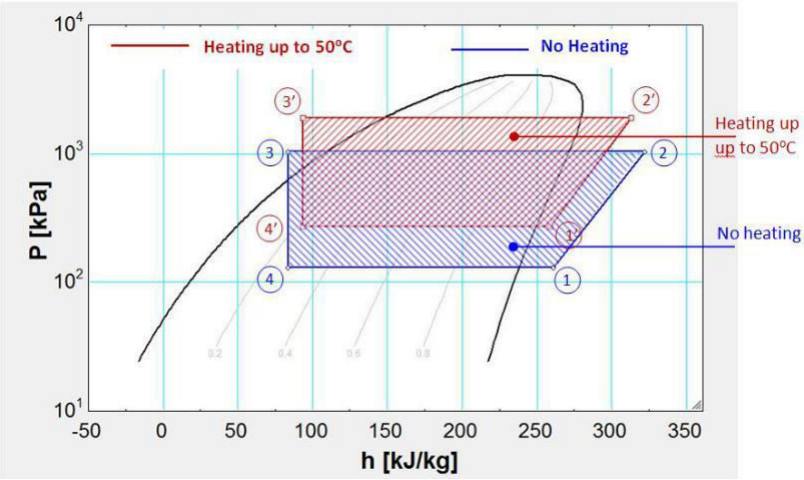

Figure 2: The pressure-enthalpy ($P-h$) diagram of the refrigeration cycle in case of no heating 1−2−3−4 and heating 1^0–2^0–3^0–4^0 the refrigerant 134a in the storage tank up to 50°C.

almost half of the pressure of R134a. This promotes R600a to be used in the refrigeration cycle that is assisted with heating than R134a due to its low operating pressure. Operating the refrigeration cycle at low pressure decreases the possibility of leakage and bursting of the pipes. From the presented results, it can be inferred that heating the refrigerant after the mechanical compressor increases temperature of the condenser as well as of the evaporator, which prevents the refrigeration cycle to be used in freezing applications in case of R134a. However, in case of R22 or R600a, temper-ature of the refrigerant at the inlet to the evaporator below the freezing temperature of water while promotes R22 and R600a to be used in freezing applications.

The subscript 2 stands for node 2 in the refrigeration cycle, which is at the inlet of the condenser.

Temperature of water in the cold water tank as a function of time and as a function of the heating process for the three types of refrigerants is shown in Fig. 3. The cooling time of water in a cold water tank is defined as the time required for cooling water from room temperature to a predetermined temperature, *i.e.* 9°C. It can be concluded based on Fig. 3a that the cooling time in case of no heating refrigerant R134a is 30 min., and this cooling time has decreased to 17 min. due to heating of the refrigerant to 50°C

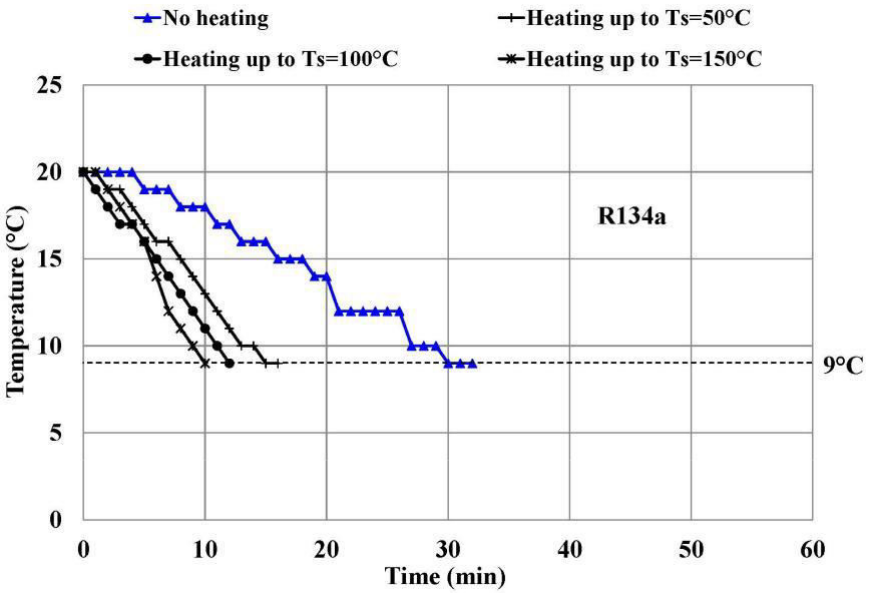

Figure 3(a)

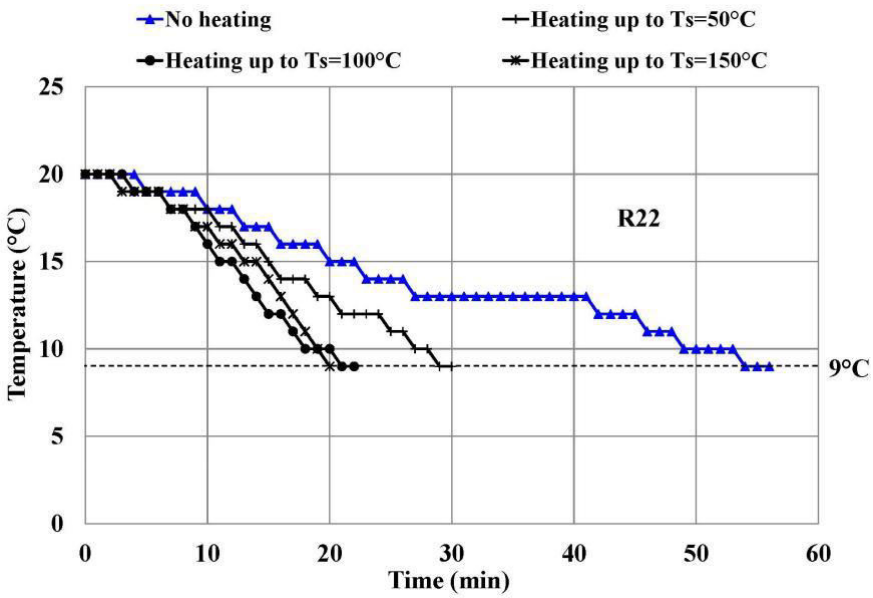

(b)

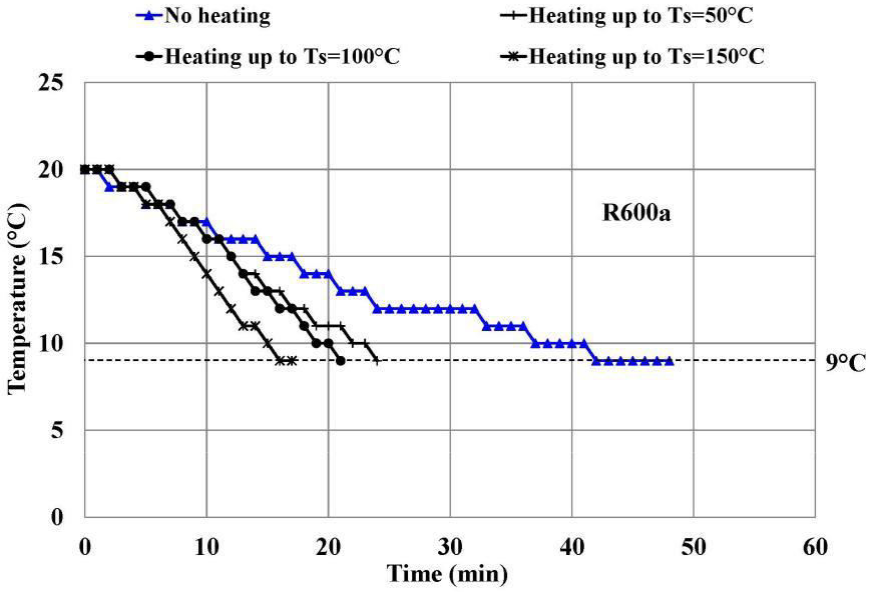

(c)

Figure 3: Temperature of water in the evaporator as a function of time and heating the refrigerant after the compressor in case of using (a) R134a, (b) R22, and (c) R600a.

after the compressor, and to 13 min. due to heating to 100°C. Heating the refrigerant after the compressor to 150°C has decreased the cooling time to 10 min. It can be seen that there is interference in the cooling curves of the water, especially at the beginning of the cooling process, and that interference diminishes as the temperature of the water approaches the set temperature. This interference is due to the uneven heating of the refrigerant in the storage tank, which results in hot spots that lingers the cooling rate and causes interference of the cooling curves. This uneven heating is so strong especially at the beginning of the heating process, however, as the temperature of the refrigerant across the storage tank stabilizes, *i.e.* becomes uniformly distributed, the difference in cooling due to different heating temperatures becomes clear.

The cooling time, t_c, as well as the cooling power, $\dot{Q}_L$, for all the examined refrigerants as well as the performed experiments are summarized in Table 3. The cooling power of the cooling cycle is equal to the heat transfer rate of the water, $\dot{Q}_{water}$, if the losses are ignored, and therefore,

$$\dot{Q}_L = \dot{Q}_{water} = \frac{m_{water} c \Delta T}{t_c}, \quad (2)$$

where m_{water} is the mass of water, c is the specific heat of water, and ΔT is temperature drop of water, such that it is cooled from 20°C to 9°C. It can be inferred from the performed experiments that heating the refrigerant after the compressor decreases the cooling time of water at the evaporator and consequently increases the cooling rate. However, the cooling rate in the case of using R134a is the highest; while in the case of R22 is the lowest at all examined temperatures. The cooling rate of R600a due to heating is intermediate between R134a and R22. The cooling power due to heating is compared to ordinary VCC, *i.e.* without heating, according to Eq. (3), and it is presented in Table 3, where the percentage increase in the cooling power, $\Delta\dot{Q}_L$, is defined as

$$\Delta \dot{Q} = \frac{\dot{Q}_{L,\,Heating} - \dot{Q}_{L,\,No\ heating}}{\dot{Q}_{L,\,No\ heating}} \times 100 \quad (3)$$

It can be concluded from Table 3 that heating the refrigerant after the compressor increases the cooling power of the cycle. Heating the refrigerant to 50°C increases the cooling power by 76.5% when using R134a, and by 69.5% when using R22, or 80% when using R600a. Also, while heating to 100°C; this increases the cooling power by 130.5% when using R134a, by

Table 3: Influence of heating the refrigerant after the compression process on the cooling rate of the refrigeration cycle for the three examined refrigerant, *i.e.* R134a, R22, and R600a.

Experiment	R134a			R22			R600a		
	t_c (min)	$\dot{Q}_L$ (kW)	$\Delta\dot{Q}_L$ (%)	t_c (min)	$\dot{Q}_L$ (kW)	$\Delta\dot{Q}_L$ (%)	t_c (min)	$\dot{Q}_L$ (kW)	$\Delta\dot{Q}_L$ (%)
No heating	30	0.153	–	56	0.082	–	48	0.10	–
Heating, T_S = 50°C	17	0.270	76.5	33	0.140	69.5	26	0.18	80
Heating, T_S = 100°C	13	0.353	130.5	22	0.200	143.9	21	0.22	120
Heating, T_S = 150°C	10	0.450	200.0	20	0.230	180.4	17	0.27	170

143.9% when using R22 and by 120% when using R600a, as well as when heating to 150°C, it increased the cooling power by 200% when using R134a, by 180.4% when using R22 and by 170% when using R600a. According to the first law of thermodynamics [42] and the energy balance during the compression process, which includes mechanical compression, $\dot{W}_{comp}$, and compression by heating at constant volume, it can be concluded that:

$$\dot{Q}_{comp} + \dot{W}_{comp} = \dot{m}_{ref} \Delta h_{comp} , \quad (4)$$

where, $\dot{m}_{ref}$, is the mass flow rate of the refrigerant and Δh_{comp} is the enthalpy change during the whole compression process, *i.e.* compression due to the mechanical compression and due to heating under constant volume, and it is equal to:

$$\Delta h_{comp} = h_2 - h_1 , \quad (5)$$

where h_1 and h_2 are the enthalpies of the refrigerant before and after the compression process, respectively. It can be indicated based on Eq. (4), that the increasing $\dot{Q}_{comp}$ and $\dot{W}_{comp}$ will increase either $\dot{m}_{ref}$ or Δh_{comp}. A detailed analysis of the refrigeration cycle is performed to determine the effect of heating on the mass flow rate or the change in enthalpy of the refrigerant through the compressor and the evaporator, which is Δh_{comp}, and Δh_{evap}, respectively. The change in enthalpy of the refrigerant through the compressor and the evaporator is presented in Table 4 as a function of the examined refrigerants and the heating temperature. It can be concluded based on Eq. (4) and the detailed analysis performed in Table 4 that the Δh_{comp} decreases with heating, which indicates that $\dot{m}_{ref}$ should increase in order to compensate for the heat energy added during the compression process. The coefficient of performance is calculated for all experiments

Table 4: Effects of heating the refrigerant after the compression process on the coefficient of performance of the refrigeration cycle for the three refrigerant types.

Experiment	R134a			R22			R600a		
	Δh_{evap} (kJ/kg)	Δh_{comp} (kJ/kg)	COP –	Δh_{evap} (kJ/kg)	Δh_{comp} (kJ/kg)	COP –	Δh_{evap} (kJ/kg)	Δh_{comp} (kJ/kg)	COP –
No heating	180.5	60.8	2.90	196.2	105.6	1.86	312.7	121.1	2.58
Heating, T_S = 50°C	167.3	54.4	3.00	18.03	97.2	1.883	302.0	111.3	2.71
Heating, T_S = 100°C	162	55.2	2.93	188.3	99.9	1.885	293.6	94.6	3.10
Heating, T_S = 150°C	159.7	55.0	2.90	185.3	94.2	1.9	297.1	95.2	3.12

Here $\Delta h_{evap} = h_1 - h_4$, $\Delta h_{comp} = h_2 - h_1$, COP = $(h_1 - h_4)/(h_2 - h_1)$.

based on the following equation:

$$\text{COP} = \frac{\dot{Q}_L}{\dot{W}_{comp} + \dot{Q}_{comp}} = \frac{\dot{m}_{ref}\,\Delta h_{evap}}{\dot{m}_{ref}\,\Delta h_{comp}} = \frac{\Delta h_{evap}}{\Delta h_{comp}}, \tag{6}$$

where $\dot{Q}_L$ is the cooling power of the refrigeration cycle. The calculated COP is presented in Table 4, and it can be seen that the variation in the COP due to heating in case of R134a and R22 is marginal, however in case of R600a is a bit a higher than the no heating case. Heating the refrigerant after the compressor under constant volume does not affect the COP of the cycle but increases the cooling power of the evaporator. According to the energy balance of the evaporator, the cooling power of the refrigeration cycle is equal to

$$\dot{Q}_L = \dot{m}_{ref}\Delta h_{evap}, \tag{7}$$

where

$$\Delta h_{evap} = h_1 - h_4, \tag{8}$$

where h_1 and h_4 are the enthalpies of the refrigerant at the outlet and inlet of the evaporator, respectively.

The mass flow rate is determined using the Eq. (9) and Table 4, and the findings are presented in Table 5. The percentage increase in the mass flow rate is calculated based on:

$$\Delta \dot{m}_{ref} = \frac{\dot{m}_{ref,\,Heating} - \dot{m}_{ref,\,No\ heating}}{\dot{m}_{ref,\,No\ heating}} \times 100 \tag{9}$$

and the results are presented in Table 5. It can be concluded that heating the refrigerant under constant volume after the compression process has a great influence on the mass flow rate, such that as the heating temper-ature increases the mass flow rate increases. Heating raises the refrigerant pressure in VCC and thereby improves the refrigerant's mass flow rate re-sulting in an improvement in the cooling capacity for the same compressor power. It can be concluded that the increase in $\dot{m}_{ref}$ due to heating un-der constant volume increases the refrigeration cooling power as have been explained by Eq. (7).

Table 5: Influence of heating the refrigerant after the compression process on the mass flow rate of the refrigerant for three refrigerant types.

Experiment	R134a		R22		R600a	
	$\dot{m}_{ref}$ (kg/s)	$\Delta\dot{m}_{ref}$ (%)	$\dot{m}_{ref}$ (kg/s)	$\Delta\dot{m}_{ref}$ (%)	$\dot{m}_{ref}$ (kg/s)	$\Delta\dot{m}_{ref}$ (%)
No heating	8.47×10^{-4}	–	4.18×10^{-4}	–	3.19×10^{-4}	–
Heating, T_S = 50°C	16.13×10^{-4}	90.440	7.70×10^{-4}	84.21	5.96×10^{-4}	86.83
Heating, T_S = 100°C	21.60×10^{-4}	155.021	10.60×10^{-4}	153.59	7.50×10^{-4}	135.11
Heating, T_S = 150°C	28.10×10^{-4}	231.760	12.40×10^{-4}	196.65	9.10×10^{-4}	185.27

5 Conclusions

It can be concluded from the performed experiments that:

1. As the heating temperature increases, the cooling power of the refrig-eration cycle increases for the same compressor power.
2. As the heating temperature increases, the temperature and pressure of the refrigerant at the inlet of the condenser increases.
3. Heating the refrigerant after the compressor under constant volume does not affect the coefficient of performance of the cycle but increases the cooling power of evaporator.
4. Heating the refrigerant after the mechanical compressor increases the temperature of the condenser as well as the temperature of the evap-orator when using refrigerant R134a, which prevents the refrigeration cycle to be used in freezing applications, however, using refrigerant R22 or refrigerant R600a promotes the heated VCC to be used in freezing applications.

5. Heating the refrigerant after the mechanical compression process in-creases the mass flow rate of the refrigerant.
6. A heated vapor compression cycle running with R600a operates at low pressures, which extends the lifetime of the operating components and decreases the chance of leakage.
7. Refrigerant R600a has the lowest operating pressure compared to R134a and R22 such that it can be used in freezing applications, and that promotes R600a as the best refrigerant to be used in heated vapor compression cycles that uses mechanical and thermal compression.
8. Heating the refrigerant after the mechanical compressor increases the cooling power of the vapor compression cycle for the same mechanical compression power. So, if solar energy is used for heating instead of electrical heating, then this will improve the cooling power of the refrigerating machine based on free energy, which decreases the energy consumption and improves the applicability of using solar energy in refrigerating machines.

Received 19 August 2020

References

[1] Dupont J.L., Domanski P., Lebrun P., Ziegler F.: *The Role of Refrigeration in the Global Economy, 38th Informatory Note on Refrigeration Technologies*. IIF-IIR, 2019.

[2] Murthy A.C., Subiantoro A., Norris S., Fukuta M.: *A review on expanders and their performance in vapor compression refrigeration systems*. Int. J. Refrig. **106**(2019), 427–446.

[3] Zhou W., Gan Z.: *A potential approach for reducing the R290 charge in air conditioners and heat pumps*. Int. J. Refrig. **101**(2019), 47–55.

[4] Luo B., Zou P.: *Performance analysis of different single stage advanced vapor compression cycles and refrigerants for high temperature heat pumps*. Int. J. Refrig. **104**(2019), 246–258.

[5] Salem M.R., El-Gammal H.A., Abd-Elaziz A.A., Elshazly K.M.: *Study of the performance of a vapor compression refrigeration system using conically coiled tube-in-tube evaporator and condenser*. Int. J. Refrig. **99**(2019), 393–407.

[6] Alahmer A., Ajib S.: *Solar cooling technologies: State of art and perspectives*. Energ. Convers. Manage. **214**(2020), 112896.

[7] Jain V., Sachdeva G., Kachhwaha S.S.: *Comparative performance study and advanced exergy analysis of novel vapor compression-absorption integrated refrigeration system*. Energ. Convers. Manage **172**(2018), 81–97.

[8] Zhu G., Chow T.-T.: *Design optimization and two-stage control strategy on combined cooling, heating and power system*. Energ. Convers. Manage **199**(2019), 111869. doi: 10.1016/j.enconman.2019.111869.

[9] Yin X., Wang X., Li S., Cai W.: *Energy-efficiency-oriented cascade control for vapor compression refrigeration cycle systems*. Energy **116**(2016), 1, 1006–1019.

[10] Alawi O.A., Salih J.M., Mallah A.R.: *Thermo-physical properties effectiveness on the coefficient of performance of Al_2O_3/R141b nano-refrigerant*. Int. Commun. Heat Mass **103**(2019), 54–61.

[11] Ahmed M.S., Abdel Hady M.R., Abdallah G.: *Experimental investigation on the performance of chilled-water air conditioning unit using alumina nanofluids*. Therm. Sci. Eng. Progress **5**(2018), 589–596.

[12] Park C., Lee H., Hwang Y., Radermacher R.: *Recent advances in vapor compression cycletechnologies*. Int. J. Refrig. **60**(2015), 118–134.

[13] Tahmasebzadehbaie M., Sayyaadi H.: *Optimal design of a two-stage refrigeration cycle fornatural gas pre-cooling in a gas refinery considering the best allocation of refrigerant*. Energ. Convers. Manage. **210**(2020), 112743.

[14] Patel D., Singh K., Jagveer.: *Improving the performance of vapor compression refrigeration system by using useful superheating*. IJESRT **3**(2014), 4, 5053–5056.

[15] Cui Z., Qian S., Yu J.: *Performance assessment of an ejector enhanced dual temperature refrigeration cycle for domestic refrigerator application*. Appl. Therm. Eng. **168**(2020), 1–10.

[16] Qureshi M.A., Bhatt S.: *Comparative analysis of cop using R134a and R600a refrigerant in domestic refrigerator at steady state condition*. Int. J. Sci. Res. **3**(2014), 12, 935–939.

[17] Jain V., Sachdeva G., Kachhwaha S.S.: *Comparative performance study and advanced exergy analysis of novel vapor compression-absorption integrated refrigeration system*. Energ. Convers. Manage. **172**(2018), 81–97.

[18] Bellos E., Vrachopoulos M.Gr., Tzivanidis C.: *Energetic and exergetic in-vestigation of a novel solar assisted mechanical compression refrigeration system*. Energ. Convers. Manage. **147**(2017), 1–18.

[19] Engineering Equation Solver (EES), http://fchartsoftware.com/ees (accessed 2 May 2021).

[20] Bellos E., Vrachopoulos M.Gr., Tzivanidis C.: *Theoretical investigation of a novel hybrid refrigeration cycle based on the partial thermal isochoric compression*. Therm. Sci. Eng. Progress **11**(2019), 239–248.

[21] Al-Alili A., Hwang Y., Radermacher R.: *Review of solar thermal air condi-tioning technologies*. Int. J. Refrig. **39**(2014), 4–22.

[22] Chen Y., Xu D., Chen Z., Gao X., Han W.: *Energetic and exergetic analysis of a solar-assisted combined power and cooling (SCPC) system with two different cooling temperature levels*. Energ. Convers. Manage. **182**(2019), 497–507.

[23] Wang J., Li S., Zhang G., Yang Y.: *Performance investigation of a solar-assisted hybrid combined cooling, heating and power system based on energy, exergy, exergo-economic and exergoenvironmental analyses*. Energ. Convers. Manage. **196**(2019), 227–241.
[24] Kwan T.H., Yao Q.: *Thermodynamic and transient analysis of the hybrid concen-trated photovoltaic panel and vapour compression cycle thermal system for combined heat and power applications*. Energ. Convers. Manage. **185**(2019), 232–247.
[25] Nehdi E., Kairouani L., Bouzaina M.: *Performance analysis of the vapor com-pression cycle using ejector as an expander*. Int. J. Energ. Res. **31**(2007), 4, 364–375.
[26] Chaiwongsa P., Wongwises S.: *Effect of throat diameters of the ejector on the performance of the refrigeration cycle using a two-phase ejector as an expansion device*. Int. J. Refrig. **30**(2007), 4, 601–608.
[27] Disawas S., Wongwises S.: *Experimental investigation on the performance of the refrigeration cycle using a two-phase ejector as an expansion device*. Int. J.. Refrig. **27**(2004), 6, 587–594.
[28] Li D., Groll E.A.: *Transcritical CO2 refrigeration cycle with ejector-expansion device*. Int. J. Refrig. **28**(2005), 5, 766–773.
[29] Elbel S., Lawrence N.: *Review of recent developments in advanced ejector tech-nology*. Int. J. Refrig. **62**(2016), 1–18.
[30] Mansuriya K., Raja B.D., Patel V.K.: *Experimental assessment of a small scale hybrid liquid desiccant dehumidification incorporated vapor compression refrigeration system: An energy saving approach*. Appl. Therm. Eng. **174**(2020), 1–14.
[31] Datta A., Halder P.: *Thermal efficiency and hydraulic performance evaluation on Ag–Al_2O_3 and SiC–Al_2O_3 hybrid nanofluid for circular jet impingement*. Arch. Thermodyn. **42**(2021), 1, 163–182.
[32] Sanaya S., Emadi M., Refahi A.: *Thermal and economic modeling and optimiza-tion of a novel combined ejector refrigeration cycle*. Int. J. Refrig. **98**(2019), 480–493.
[33] Bellos E., Tzivanidis C.: *Alternative designs of parabolic trough solar collectors*. Prog. Energ. Combust. **71**(2019), 81–117.
[34] Chou D., Chang C., Chang J.: *Energy conservation using solar collectors inte-grated with building louver shading devices*. Appl. Therm. Eng. **168**(2016), 1282– 1294.
[35] El Mahallawy N., Aref F.A., Abd-Elhady M.S.: *Effect of metallic reflectors and surface characteristics on the productivity rate of water desalination systems*. Therm. Sci. Eng. Progress **17**(2020), 100489.
[36] AL-Joboory H.N.S.: *Experimental and theoretical investigation of an evacu-ated tube solar water heater incorporating wickless heat pipes*. Arch. Thermodyn. **41**(2020), 1, 3–31.
[37] Abdolhossein Zadeh A., Nakhjavani S.: *Thermal analysis of a gravity-assisted heat pipe working with zirconia-acetone nanofluids: An experimental assessment*. Arch. Thermodyn. **41**(2020), 2, 65–83.
[38] Dubba S.K.: *Flow of partially condensed R-134a vapor through an adiabatic capil-lary tube*. Flow Meas. Instrum. **59**(2018), 1–7.

[39] Digital K-Type Thermometer, http://www.meter-depot.com (accessed 2 May 2020).

[40] Pico Technology, http://www.picotech.com (accessed 2 May 2020).

[41] Abd-Elhady M.S., Bishara E., Halim M.A.: *Increasing the cooling rate of the vapor compression cycle by heating*. Int. J. Air-Cond. Refrig. **29**(2021), 1, 2150009.

[42] Cengel Y.A., Boles M.A.: Thermodynamics: An Engineering Approach (6th Edn.). McGraw Hill, 2008.